Ab-initio calculation of positron annihilation rates in solids

1991 J. Phys.: Condens. Matter 3 3455

(http://iopscience.iop.org/0953-8984/3/20/007)

J. Phys.: Condens. Matter 3 (1991) 3455–3469. Printed in the UK

Ab-initio calculation of positron annihilation rates in solids

M J Puska

Laboratory of Physics, Helsinki University of Technology, 02150 Espoo, Finland

Received 21 November 1990, in final form 28 February 1990

Abstract. Recently, Jensen showed that the positron annihilation rates in metals can be calculated rather successfully within the local-density approximation (LDA) using the total electron density as the only input. Thus, the division into core, valence, and, in the case of transition metals, the d electrons, is not necessary. Jensen calculated the positron lifetimes on the basis of non-self-consistent electron structures. We have calculated in this work positron annihilation rates using self-consistent electron structures. The use of self-consistent electron densities makes the LDA lifetimes longer and, especially in the case of simple metals, a better agreement with experimental results is obtained. In this article we present results for several simple and transition metals and study the trends along the different columns and rows of the Periodic Table. Moreover, we have calculated the positron annihilation rates also for semiconductors using a slightly different enhancement function. The reasons for the success of the LDA are discussed and the implications to the calculation of lifetimes for positrons trapped at crystal defects are demonstrated by examples.

1. Introduction

During the last decade we have been witnessing the rapid development of the *ab-initio* modelling of solids on the basis of the density-functional theory [1]. Most of the important basic properties of solids, such as the cohesive properties, can be calculated without any adjustments to the experimental results. Moreover, in many cases it is possible to predict by calculations values for quantities that sometimes probe in a very indirect way the atomic and electronic structures of solids, and thereby calculations give essential support for the analysis of the experimental data. This is also the prevailing situation in the case of positron annihilation [2].

The basis for the calculation of positron states in solids is the two-component density-functional theory [3]. In this theory all the ground-state properties of the electron–positron system in an external field can be determined from functionals depending on the electron and positron densities. The idea of the two-component density-functional theory is that the system of interacting particles can be described as a system of non-interacting particles by introducing exchange and correlation functionals. When the local density approximation (LDA) is made for these functions, average electron and positron densities are easily solved by minimizing the total energy functional. The meaning of the exchange and correlation for electrons is that the electron density is depleted around a given electron due to Pauli principle and Coulomb repulsion (exchange–correlation hole). In the case of positrons the normal

0953-8984/91/203455+15$03.50

experimental situation is that there is only one positron in the sample at a given time. This means that the exchange effects for a positron delocalized in the whole sample vanish. The Coulomb correlation means that there is a pile-up of electrons around the positron. The attractive Coulomb interaction between an electron and its exchange–correlation hole gives the electron exchange and correlation energy. Correspondingly the Coulomb interaction connected with the positron and its screening cloud gives the positron correlation energy. In LDA these energies are calculated as spatial integrals from functions which at a given point depend only on the electron density at that point. The energy-density functions needed are known from the calculations for the homogeneous electron gas [4].

A natural continuation to the above picture is that the positron annihilation rate, i.e. the inverse of the positron lifetime, is calculated within LDA, too. This was recently suggested by Jensen [5]. The annihilation rate is directly proportional to the contact electron density at the positron. LDA for the annihilation rate means that the contact electron density, including the average density and the pile-up (enhancement) due to correlation, depends at a given point on the total electron density at that point. The total annihilation rate is obtained again as a spatial integral and the enhancement at a given point is obtained from the data for the positron in the homogeneous electron gas [3]. Jensen [5] applied the LDA scheme for several metals using non-self-consistent electron densities as the starting point. His calculation gave rather systematically about 10% shorter lifetimes than the measured ones. We show below that the use of self-consistent electron densities increase the positron lifetimes and in the case of simple metals the discrepancy between experimental and theoretical results is actually removed. Moreover, the calculations using self-consistent electron structures avoid the arbitrariness connected with the atomic configurations which have to be chosen according to some criteria when constructing non-self-consistent electron structures [6]. This is an important benefit for the systematic studies of trends along the rows of Periodic Table.

Previously [7], we have calculated the total annihilation rates for positrons in solids by dividing the electron density into core, valence, and possibly also d level contributions and using constant enhancement factors for the positron annihilation with core and d level electrons and a density-dependent enhancement (in LDA) for valence electrons only. The new LDA formulation is preferable because it is in accordance with the density-functional theory, which states that the *total* densities are the physical quantities and in principle a division into different density contributions is not justified. Moreover, the old formulation leads to somewhat arbitrary constant enhancement factors for the core and d level annihilations, the latter of which has been used as an adjustable parameter in order to reproduce the experimental positron bulk lifetimes (lifetimes for delocalized positrons in a perfect crystal). In contrast, the LDA formulation is a pure *ab-initio* method without any adjustable parameters and should therefore have a much larger predictive power than the old formulation.

In this work we test the LDA scheme by calculating positron lifetimes for most common metals, group-IV, and III–V compound semiconductors. The self-consistent electron structures for the perfect periodic solid lattices are obtained by the linear-muffin-tin-orbital method (LMTO) within the atomic-spheres approximation (ASA) [8]. The positron states are also calculated with the same method. We have already applied the LDA scheme and these numerical methods for the calculation of positron energetics (i.e. positron affinity, deformation potential, positron work function, and positronium formation potential) for the same metals as in this work [9, 10]. The great benefit of

this kind of *ab-initio* calculation is that they enable systematic studies to be made of trends along the rows and columns of the Periodic Table, and thereby increase our understanding of positron properties in different systems. In this work we investigate also how the new LDA affects the former pictures we have for annihilation of positrons trapped at crystal defects. For this purpose we calculate the self-consistent electron structures and positron states for vacancies in Al and GaAs by the Green's function method [11, 12] corresponding to LMTO-ASA. The results are compared with those obtained by applying LDA in the three-dimensional superimposed atom method [7].

2. Theory

For a positron delocalized in a perfect crystal the two-component theory attains a very simple form, because the positron density at each point is vanishingly small, and does not affect the average electron density. This is the zero-positron-density limit of the theory. In this case the electron structure is first determined self-consistently with some standard band-structure code. Thereafter the potential $V(\boldsymbol{r})$ felt by positron is obtained in LDA as

$$V(\boldsymbol{r}) = V_{\mathrm{Coul}}(\boldsymbol{r}) + V_{\mathrm{corr}}(n_{-}(\boldsymbol{r})) \tag{1}$$

where $n_{-}(\boldsymbol{r})$ and $V_{\mathrm{Coul}}(\boldsymbol{r})$ are the self-consistent electron density and the Coulomb potential due to the nuclei and the electron density $n_{-}(\boldsymbol{r})$. $V_{\mathrm{corr}}(n)$ is the positron–electron correlation energy, which is due to the formation of the screening electron cloud around the positron and it is calculated for a delocalized positron in a homogeneous electron gas with density n. The above potential is inserted into the same code which is used in the calculation of the electron structures and the solution with the lowest energy is the ground state of the positron in the perfect crystal.

Once the positron and electron densities have been found, the total positron annihilation rate can be determined from their overlap. Here one has to take into account the pile-up or enhancement of the electron density at the positron. In LDA the total positron annihilation rate λ reads as

$$\lambda = \int \mathrm{d}\boldsymbol{r}\; n_{+}(\boldsymbol{r})\Gamma(n_{-}(\boldsymbol{r})) \tag{2}$$

where $n_{+}(\boldsymbol{r})$ is the positron density and $\Gamma(n)$ is the positron annihilation rate in a homogeneous electron gas with density n. Recent many-body calculations result in the following interpolation form for $\Gamma(n)$ [3]:

$$\Gamma(n) = \pi r_0^2 cn(1 + 1.23r_s + 0.8295r_s^{3/2} - 1.26r_s^2 + 0.3286r_s^{5/2} + \tfrac{1}{6}r_s^3). \tag{3}$$

Above, r_0 is the classical electron radius, c is the velocity of light and $r_s = (\frac{3}{4\pi}n)^{1/3}$ is the usual electron density parameter. In equation (3) the prefactor $\pi r_0^2 cn$ is the independent-particle model (IPM) result for the annihilation rate. The part inside the brackets defines the so-called (density-dependent) enhancement factor. In equation (3) it is assumed that the positron is completely screened by electrons and therefore the use of LDA with equation (3) is valid for *metals*.

In semiconductors or insulators the positron screening by electrons is not perfect due to the existence of the band gap. This has to be taken in account in the electron–positron correlation energy and in the annihilation rate. In the case of *semiconductors*

we rely on the semiempirical formulation presented in [13]. The formulation leans on the results for the homogeneous electron gas. The annihilation rate (3) has to be substituted with

$$\Gamma(n) = \pi r_0^2 cn[1 + 1.23r_s + 0.8295r_s^{3/2} - 1.26r_s^2 + 0.3286r_s^{5/2} + \tfrac{1}{6}(1 - 1/\epsilon_\infty)r_s^3] \qquad (4)$$

where ϵ_∞ is the high-frequency dielectric constant. The form of equation (4) can be justified by two constraints for the screening cloud of the positron [13]. Firstly, at the positron ($r = 0$) the electron density $n(r)$ obeys the cusp condition

$$(\partial n/\partial r)|_{r=0} = -n(0). \qquad (5)$$

Secondly, the screening cloud $\Delta n(r)$ induced by the positron has to contain $(1 - \frac{1}{\epsilon_\infty})$ electrons, i.e.

$$\int_0^\infty \Delta n(r) 4\pi r^2 \, dr = \left(1 - \frac{1}{\epsilon_\infty}\right). \qquad (6)$$

This guarantees that the Coulomb potential due to positron is the long range potential proportional to $\frac{1}{\epsilon_\infty r}$. The effects due to the reduced screening on the correlation potential are less pronounced and they can be taken into account by noting that the correlation potential scales as $\sim (\lambda - \lambda_0)^{1/3}$ [14], where λ is the actual annihilation rate and λ_0 is the IPM result. In the case of insulators the screening efficiency of the valence electrons is reduced due to the larger band gaps from that for metals, more than in the case of semiconductors. Therefore the semiempirical formulation (equation (4)) based on positron screening in free electron gas is no longer adequate. For insulators one could use, for example, the formalism presented in [13], but it is based on fitting to experimental positron bulk lifetimes and thus it is not an *ab-initio* method.

In the present work we obtain the self-consistent electron structures for the perfect periodic lattices by the LMTO-ASA method [8]. For the vacancies we employ the corresponding Green function method [11, 12]. In the ASA the lattices are divided into space-filling spheres, centred at host nuclei and in the case of diamond- or zincblende-structure semiconductors spheres centred around the tetrahedral interstitial sites are used, too. Use of the ASA means also that potentials and charge densities are spherical averages within these spheres. The ASA violates the actual three-dimensional geometry most strongly in the interstitial regions near the sphere surfaces. This violation is, however, not severe for the electron states [15], and experience [12, 2, 9] as well as the results presented below show that this holds also for the positron states. More important is that the electron density is determined self-consistently. In fact, in the case of positron energetics in LDA [9, 10], the ASA has the great benefit that it provides a unique energy reference level for electrons and positrons.

3. Results and discussion

Positron bulk lifetimes calculated in the LDA for elemental metals and semiconductors Si, Ge, and Sn are shown in figure 1. Bulk lifetimes for nine III–V compound semiconductors are given in figure 2. The lattice constants correspond to 300 K, except those for alkaline metals, and the values used in actual calculations are given in [9]

and [13] for metals and non-metals, respectively. In the case of metals only BCC and FCC structures are used, i.e. the hexagonal structures are substituted with FCC ones with the same Wigner–Seitz radii. Diamond or zincblende structures are used for all semiconductors. The electron structures are spin-compensated and scalar-relativistic in all cases. Moreover, the frozen-core approximation is employed, i.e. only the valence electrons (including the uppermost d electrons for transition and noble metals as well as for Zn, Cd, and Hg) are allowed to relax from their free atom distributions.

Positron Bulk Lifetime (ps)

Li 305	Be 137												
Na 337	Mg 237											Al 166	Si 221
K 387	Ca 297	Sc 199	Ti 146	V 116	Cr 101	Mn 103	Fe 101	Co 97	Ni 96	Cu 106	Zn 134		Ge 228
Rb 396	Sr 319	Y 219	Zr 159	Nb 122	Mo 111	Tc 95	Ru 90	Rh 93	Pd 103	Ag 120	Cd 153		Sn 275
Cs 407	Ba 315	Lu 199	Hf 149	Ta 117	W 100	Re 91	Os 86	Ir 87	Pt 94	Au 107			Pb 187

Figure 1. Calculated positron bulk lifetimes τ (ps) for elemental metals and group-IV semiconductors. The lattice structures and lattice constants used in the calculations are given in [9].

		ANION		
		P	As	Sb
CATION	Al	226	233	263
	Ga	219	230	256
	In	246	255	278

Figure 2. Calculated positron bulk lifetimes τ (ps) for nine III-V compound semiconductors. All compounds have the zinc blende lattice structure and the lattice parameters and dielectric constants used are given in [13].

The calculated positron bulk lifetimes for metals vary from 86 ps (Os) to 407 ps (Cs). The trends seen in the lifetimes along the 3d, 4d and 5d rows of the Periodic Table are very similar to the behaviour of the Wigner–Seitz radii. The positron lifetime is longest for the alkali metals and decreases thereafter rapidly towards the centre of the d series in question. Around the middle of a series the positron lifetimes vary only little between the adjacent elements and thereafter the lifetime rises slightly towards the noble metals. The similar behaviour of the positron bulk lifetime and the Wigner–Seitz radius reflects the importance of the size of the open interstitial volume and the corresponding interstitial electron density in determining the total positron annihilation rate (see below). In the case of diamond- or zincblende-structure semiconductors this conclusion is even more evident from the strong correlation between the effective electron density seen by the positron and the unit cell volume of the lattice [13].

Experimental positron bulk lifetimes have been collected for example in [16] and [13]. The present LDA values for the transition metals are maybe slightly shorter

than the measured ones. In the case of simple metals and semiconductors agreement with experiments is generally better. The comparison is, however, somewhat difficult, especially if one is interested in the small details in the trends between different metals and semiconductors, because the lifetimes quoted originate from different sources and the measured lifetime for one particular metal or semiconductor may vary even by 10 ps or more. The reasons for these variations may lie in the sample preparation (annealing), in timing devices (e.g. lifetime spectrometers with BaF_2 seem to give systematically smaller lifetimes than those with plastic scintillators [17]), or in the data analysis (where the so-called source corrections play an important role). In order to give the reader some idea on the predictive power of the LDA *ab-initio* method, but to avoid the above described difficulties in comparison, we give in table 1 positron bulk lifetimes [18] measured recently using the same experimental set-up (plastic scintillators) and analysed with the same methods. The present LDA results are also given in table 1. The theoretical lifetimes for the transition metals given are about 10 ps shorter than the experimental ones, whereas in the case of semiconductors the theoretical lifetimes are maybe slightly too long. However, it is gratifying to note that the relative differences between the 3d metals Fe, Ni, and Cu are very similar both according to measurements and calculations.

Table 1. Measured positron bulk lifetimes τ^{exp} [18] compared with present theoretical values τ^{theor}. In the experiments [18] the samples have been carefully annealed before measuring with a conventional plastic scintillator fast–fast positron lifetime spectrometer. A ^{22}Na positron source inside Ni foil has been sandwiched between two sample pieces. The lifetime spectra have been analysed with one lifetime component after source corrections.

Host	τ^{exp} (ps)	τ^{theor} (ps)
Fe	112	101
Ni	107	96
Cu	120	106
Si	216	221
GaAs	231	231
InP	244	247

We have calculated the positron bulk lifetimes also for the II–IV compound semiconductors CdTe and HgTe and for the insulators C (diamond), GaN, MgO, and SiC using the above described semiempirical model (equation (4)) for screening. The lattice data used are given in [13]. The calculated lifetimes 282 ps and 261 ps for CdTe and HgTe, respectively, are somewhat shorter than the experimental ones collected in [13]. However, one should note that the theoretical values depend on the dielectric constant. The dielectric constant, on the other hand, can vary considerably as a function of composition in the actual samples, which are usually ternary compounds of the type $Cd_xHg_{1-x}Te$. Therefore the conclusion is that LDA seems to be able to describe the annihilation also in these II–VI compounds, where the annihilation with the uppermost cation d electrons is important. The calculated positron bulk lifetimes for C, GaN, MgO, and SiC are 95, 158, 125, and 142 ps, respectively. With the exception of MgO these values are considerably lower than the experimental bulk lifetimes quoted in [13]. Thus, it is obvious that the screening model of equation (4) based on the properties of the free electron gas cannot describe the electron enhancement in

wide-gap insulators.

In order to further analyse the positron annihilation characteristics in solids and in order to be able to compare with previous theoretical works, we divide the total annihilation rate λ (equation (2)) into core (λ_c) and valence components (λ_v) as suggested by Jensen [5]. That is,

$$\lambda_c = \int dr\, n_+(r)\Gamma(n_-(r))\frac{n_c(r)}{n_-(r)} \qquad \lambda_v = \int dr\, n_+(r)\Gamma(n_-(r))\frac{n_v(r)}{n_-(r)} \tag{7}$$

where n_c and n_v are the densities corresponding to the core and valence electron levels. In the case of transition metals we treat the uppermost d electrons as valence electrons, because due to the sd hybridization the division to s and d valence electrons is ambiguous. As a matter of fact, the division of the total electron density into components with physical meaning is not, in principle, possible in the density-functional theory. Further, following Jensen we define the enhancement factors for the core and valence annihilations as

$$\gamma_c = \frac{\lambda_c}{\lambda_c^{IPM}} \qquad \gamma_v = \frac{\lambda_v}{\lambda_v^{IPM}} \tag{8}$$

where λ_c^{IPM} and λ_v^{IPM} are the core and valence annihilation rates in IPM, i.e. they are calculated in equation (7), but $\Gamma(n)$ is substituted by

$$\Gamma^{IPM}(n) = \pi r_0^2 cn. \tag{9}$$

In the above definitions it is assumed that the enhancement factors do not depend on the energy of the electron participating in the annihilation. However, according to theory and experiments the enhancement increases as a function of the electron energy [19]. Therefore the enhancement factors (8) are average quantities, and in particular the core enhancement factors obtained are upper estimates of the true factors. Similarly, the true core annihilation rates would be lower than those calculated with equation (7). One should also note that following Jensen we have calculated the IPM annihilation rates using a positron wavefunction, which corresponds to the total potential (1). In [6], for example, the IPM rate is calculated from a wavefunction, which is constructed without the correlation potential. We have calculated that the use of the latter definition would increase the present core enhancement factors by of the order of 10% whereas the effect on the valence enhancement factors is smaller.

The partial annihilation rates and the enhancement factors obtained in this work are collected in table 2. In the 3d and 5d series the core annihilation rate has a parabolic shape with the maxima in the middle of the series at Cr and W, respectively. In the case of 4d series there is a shallow local minimum in the middle at Mo. The increase of the core annihilation rate to the right in the beginning of the d series means the increase of the overlap of positron and core-electron densities. This is due to the shrinkage of the interstitial open volume since the Wigner–Seitz radius decreases strongly whereas the size of the repulsive core region decreases more slowly. The decrease of the Wigner–Seitz radius results from the filling of the bonding d orbitals. In the latter half of the d series anti-bonding d orbitals are being filled and the Wigner–Seitz radius is nearly constant. The core electrons become more strongly bound when the nuclear charge increases and thus the core annihilation rate decreases. In each d series the valence annihilation rate is seen to increase as a function of the

nuclear charge until a slight drop at the end of each series. The increasing trend reflects the increase of the electron density in the interstitial region when filling the d levels. The opposite behaviour of the core and valence annihilation rates in the latter half of the d series compensate each other in the total annihilation rate and therefore the variations in the positron lifetimes between different metals are rather small in these regions of the Periodic Table, as can be seen from figure 1.

Table 2. Calculated positron annihilation characteristics for perfect crystal lattices. Positron annihilation rates with core (λ_c) and valence (λ_v) electrons, and the core (γ_c) and valence (γ_v) enhancement factors are given. λ_c, λ_v, γ_c, and γ_v are defined in equations (7)–(9).

Host	λ_c (ns^{-1})	λ_v (ns^{-1})	γ_c	γ_v
Li	0.382	2.896	3.263	7.997
Be	0.577	6.711	2.292	3.619
Na	0.568	2.401	3.713	11.170
Mg	0.525	3.704	2.867	5.557
Al	0.504	5.520	2.484	4.047
Si	0.138	4.388	2.251	4.490
K	0.559	2.028	5.927	18.212
Ca	0.617	2.754	3.969	7.788
Sc	1.129	3.894	3.104	4.825
Ti	1.672	5.173	2.753	3.863
V	2.052	6.553	2.537	3.403
Cr	2.166	7.723	2.406	3.178
Mn	1.753	7.923	2.325	3.178
Fe	1.684	8.261	2.263	3.118
Co	1.590	8.698	2.193	3.053
Ni	1.460	8.915	2.132	3.019
Cu	1.127	8.308	2.092	3.107
Zn	0.598	6.851	2.070	3.437
Ge	0.405	3.983	2.411	4.866
Rb	0.610	1.917	6.904	20.889
Sr	0.635	2.499	4.550	9.037
Y	1.089	3.476	3.431	5.260
Zr	1.540	4.751	2.961	4.055
Nb	2.017	6.165	2.701	3.482
Mo	1.912	7.075	2.584	3.307
Tc	2.159	8.414	2.446	3.077
Ru	2.051	9.064	2.370	3.000
Rh	1.771	8.950	2.329	3.017
Pd	1.401	8.324	2.293	3.102
Ag	0.961	7.328	2.259	3.285
Cd	0.509	5.990	2.245	3.690
Sn	0.387	3.248	2.699	6.294
Cs	0.654	1.803	8.436	25.136
Ba	0.897	2.276	4.886	9.185
Lu	1.330	3.708	3.141	4.886
Hf	1.699	5.025	2.796	3.923
Ta	2.073	6.498	2.584	3.424
W	2.172	7.840	2.466	3.175
Re	2.135	8.850	2.378	3.044
Os	2.027	9.650	2.311	2.959
Ir	1.741	9.784	2.267	2.953
Pt	1.413	9.205	2.250	3.017
Au	1.022	8.301	2.221	3.143
Pb	0.191	5.167	2.164	4.127

The core enhancement factors given in table 2 decrease monotonically to the right along each d series. At the beginning of a series the decrease is very steep whereas at the end the rate is small. The decrease reflects the strengthening of bonding of the core electrons to the nucleus as the nuclear charge increases. The valence enhancement factors are very large for the alkaline metals and decrease to the right in the Periodic Table. The decrease is strong at the beginning of a series but declines very rapidly. At the end of each series the valence enhancement factor increases slightly. The behaviour of the valence enhancement factor is directly correlated with the enhancement of the electron density at the positron in a free electron gas. This is given by the contents of the brackets in equation (3), which indicates that the enhancement increases strongly when the electron gas density decreases (r_s increases).

Previously, the core annihilation rates for alkaline, 3d transition, and some 4d transition metals have been calculated by Šob [20]. First he calculated the core an-

nihilation rates in IPM using non-self-consistent electron structures. Thereafter he used a constant core enhancement factor determined for every metal in a semiempirical model, which related the core enhancement factor to the core polarizability. The trends obtained by Šob for the core annihilation rates are in a good agreement with the present results. In the case of the 3d metals his absolute values are larger than the present ones at the beginning of the series and smaller at the end of the series. The core enhancement factors obtained by Šob also obey the same trends as the present results. His absolute values for the 3d transition metals are in most cases slightly smaller and for 4d transition metals slightly larger than our values in table 2. However, the agreement is astonishing, because Šob's model for the core enhancement factors differs totally from the present approach.

Jensen [5] has calculated positron bulk lifetimes for several metals using the LDA description. The main difference between his calculations and the present ones is that he used non-self-consistent electron structures based on atomic superposition. Further, in order to solve the positron wavefunction and to calculate the annihilation rate he used the Wigner–Seitz approximation with spherically averaged potential and charge densities. The general trend is that Jensen's lifetimes are about 3–6 ps shorter than ours in this work. In the case of alkali metals the differences are, however, much more important, i.e. 10–25 ps. Due to this difference our results for the alkaline metals are in much better agreement with measurements than Jensen's predictions. As will be discussed below, the too short positron lifetimes for alkali metals in Jensen's calculations result from the use of non-self-consistent electron structures. The other differences are presumably due to numerical approximations. Jensen gives also the core, d level, and valence electron enhancement factors. His core enhancement factors are consistently lower than ours but his valence annihilation factors for simple metals, for which the comparison is possible, are in very good agreement with our results. The good agreement in the case of the valence enhancement factors results simply from the fact that the valence electron enhancement is mainly determined by the enhancement for the free electron gas in equation (3).

Very recently Daniuk *et al* [6] have also made *ab-initio* calculations for positron annihilation rates in metals. However, their approach cannot be justified on the basis of density-functional formalism. They calculated the core annihilation rate using the zero-momentum limit of the electron–positron momentum-dependent enhancement factor for homogeneous electron gas. Moreover, this enhancement was calculated in the LDA, i.e. at a given point it depends on the total density at that point. The valence annihilation rate was calculated in their approach in the same way as in this work or in Jensen's work (equations (7) and (4)). Daniuk *et al* obtained the spherical Coulomb potentials around a nucleus in a solid by applying the Mattheiss construction. For the electron densities they used atomic wavefunctions either from free atom configurations or from the so-called solid-state configurations. The core annihilation rates obtained by Daniuk *et al* agree well with the present ones: at the beginning of each d series their values are slightly larger than ours and the ordering changes towards the end of the series. Their valence annihilation rates are consistently about 5% lower than ours. This difference is presumably mainly due to different numerical approaches in constructing the valence electron densities.

In order to study effects connected to the self-consistency of electron densities and effects due to approximations (ASA) in the lattice geometry, we have performed positron state calculations with non-self-consistent electron structures using the LMTO-ASA method and the three-dimensional superimposed atom method [7]. The positron

potential and electron density for the LMTO-ASA method have been calculated by superimposing free atom Coulomb potentials and charge densities and performing thereafter the spherical averaging. In the three-dimensional superimposed atom method the electron density and the potential sensed by positron are constructed by overlapping free atoms. Thereafter the positron wavefunction is solved from a three-dimensional Schrödinger equation by a relaxation method and the positron annihilation rate is calculated by a three-dimensional integration. The results from these calculations for Al, K, Fe, Cu, and Si are shown in table 3. The results obtained by the LMTO-ASA method (NSC-ASA) are in a good agreement with those obtained by Jensen [5] reflecting the fact that the approaches beyond the numerical details are identical. When compared with the self-consistent results given in figure 1 and in table 2 the non-self-consistent results show larger core annihilation rates. In the case of Al and transition metals Fe and Cu the larger core annihilation rates are compensated by the decrease of the valence annihilation rates and the positron lifetimes do not essentially change. But in the case of K and Si this kind of compensation is less perfect and the self-consistency of the electron structure increases the positron lifetime remarkably. Figures 3 and 4 clarify the situation further in the case of Fe. Figure 3 shows the spherically averaged self-consistent and non-self-consistent radial valence electron densities ($4\pi r^2 n(r)$). It can be seen that there is a transfer of electron density from the core region to the interstitial bond region when free atoms form the solid. This charge transfer lowers the self-consistent potential for the positron in the interstitial region and raises it in the core region, as can be seen from figure 4. As a result, the positron wavefunction in the self-consistent case is reduced in the core region and enhanced in the interstitial region relative to the one calculated using a non-self-consistent electron density. Thus, the positron density follows the relaxing electron density. The electron charge transfer and the changes in wavefunction decrease the core and increase the valence annihilation rate.

Table 3. Positron annihilation characteristics for perfect Al, K, Fe, Cu, and Si lattices. The results are obtained by using non-self-consistent electron structures in the LMTO-ASA method (NSC-ASA) or in the fully three-dimensional superimposed atom method (NSC-3D) [7]. Positron annihilation rates with core (λ_c) and valence (λ_v) electrons, positron lifetimes (τ), and the core (γ_c) and valence (γ_v) enhancement factors are given. λ_c, λ_v, γ_c, and γ_v are defined in equations (7) - (9).

Method	Host	λ_c (ns^{-1})	λ_v (ns^{-1})	τ (ps)	γ_c	γ_v
NSC-ASA	Al	0.643	5.411	165	2.337	4.085
	K	0.768	1.970	365	4.733	18.063
	Fe	1.946	7.970	101	2.212	3.108
	Cu	1.281	8.177	106	2.052	3.077
	Si	0.146	4.538	214	2.187	4.414
NSC-3D	Al	0.611	5.340	168	2.342	4.125
	K	0.752	1.970	367	4.765	18.464
	Fe	1.854	7.682	105	2.222	3.155
	Cu	1.241	7.953	109	2.057	3.108
	Si	0.142	4.441	218	2.201	4.485

Comparing the results obtained by the LMTO-ASA (NSC-ASA) and the three-dimensional superimposed atom method (NSC-3D) one can conclude that the effects

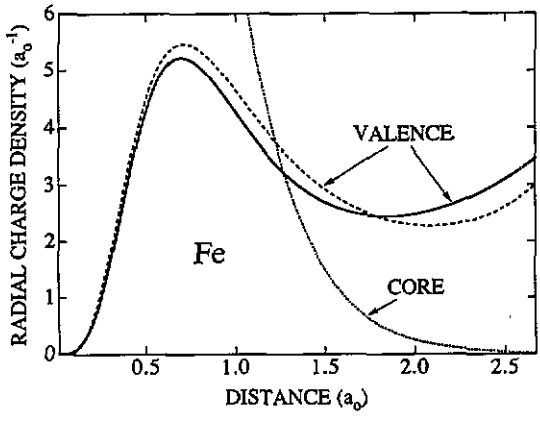

Figure 3. Radial charge densities ($4\pi r^2 n(r)$) around a nucleus in BCC Fe. The self-consistent valence charge density (full curve) is obtained by the LMTO-ASA method. The non-self-consistent valence charge density (broken curve) is obtained by superimposing free atom densities and averaging spherically the resulting three-dimensional density around a nucleus. The core electron density (chain curve) is shown, too.

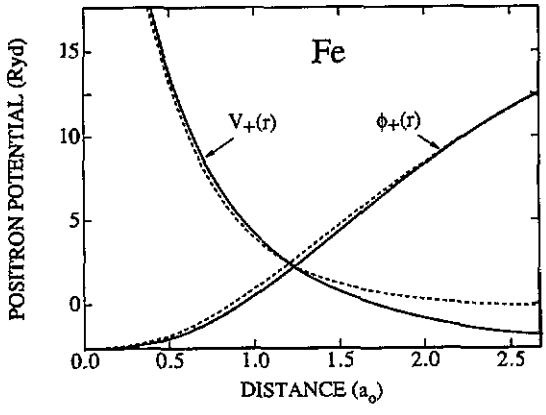

Figure 4. Positron potential $V_+(r)$ and corresponding positron wavefunction around a nucleus in BCC Fe. The self-consistent potential (full curve) is obtained by using in equation (1) the self-consistent electron density and Coulomb potential calculated by the LMTO-ASA method. The non-self-consistent potential (broken curve) is obtained by using the superimposed and spherically averaged electron density and Coulomb potential. The corresponding positron wavefunctions (full curve for the self-consistent potential and broken curve for the non-self-consistent potential) are also calculated by the LMTO-ASA method.

due to the geometry violation in the ASA are rather small. The net effect is that the more accurate treatment of the geometrical shape of the Wigner–Seitz cell and the electron and positron densities increases the positron lifetime by a few picoseconds.

Previously we have calculated positron lifetimes in the model of superimposed atoms by treating the annihilation with core, d level, and valence electrons separately [7,2]. For the core enhancement factor we used the rather low value of $\gamma_c = 1.5$, which is supported by the theory explaining core enhancement at the high-electron-momentum region in the positron angular correlation measurements [21]. The enhancement factor for the uppermost d level electrons was used as an adjustable pa-

rameter to give the experimental positron lifetimes for the transition metals. Finally, the semiempirical Brandt–Reinheimer form [22] was used for the positron annihilation with valence electrons. In the case of simple metals, elemental semiconductors, and III–V semiconductors this scheme has no adjustable parameters. However, it predicts the experimental positron bulk lifetimes rather accurately [7, 23, 13]. In the light of the present results this success is due to effects which compensate each other: the use of too low a core enhancement factor decreases the core annihilation rate, whereas the lack of self-consistency in the electron densities increases it. Moreover, the semiempirical Brandt–Reinheimer formula contains a contribution from the core electrons, and therefore it overestimates the valence annihilation rate. (The Brandt–Reinheimer formula may not be used instead of equation (3); it leads to too low positron lifetimes due to the double counting of core annihilation rates.)

In order to demonstrate the predictive power of the new LDA approach also in the case of positrons trapped at vacancy-type defects in solids, we have performed calculations for vacancies in the FCC metal Al and in III–V semiconductor GaAs. According to the two-component density-functional theory [3] the electron and positron densities should be solved simultaneously self-consistently when the positron wavefunction is localized. This is because the localized positron affects the electron density also on the *average* level besides the short-range screening, which is the only effect in the case of a delocalized positron. In this work however, we rely on the usual scheme, which is similar to the scheme valid rigorously only for the delocalized positron states. We first calculate the self-consistent electron structure for the vacancy without the influence of the localized positron. Thereafter the positron potential is constructed within the LDA, the localized positron state is solved, and finally the positron annihilation rate is calculated by taking the short-range screening, or the enhancement, into account as in the case of delocalized positrons. The use of the approximative scheme can be justified, because it gives similar results for the positron annihilation rates to the full two-component theory [3, 24]. This similarity results from cancellation of two effects: in the approximative scheme the average electron density at the defect is lower than in the fully self-consistent two-component scheme, but the short-range electron enhancement at the positron is then larger in the former scheme due to the lower average electron density. The calculations for vacancies employ in this work the self-consistent LMTO-ASA Green function method [11]. This method introduces a further approximation, namely, lattice relaxation around the defect is not taken into account, but the ions around the vacancies sit at their perfect crystal positions.

The results for positron lifetimes in vacancies are collected in table 4. The use of LDA makes the calculated lifetimes shorter than those [7, 13] calculated by treating the core and valence annihilations separately. The same trend was noted also by Jensen [5], who calculated the positron lifetimes for vacancies in Cu and Mo using the superimposed atom method. The self-consistent electron structures lead to longer positron lifetimes than the non-self-consistent ones, similarly to the case of bulk lifetimes. However, the differences are now smaller, because of the reduced importance of the core annihilation. Different charge states are possible for vacancies in semiconductors, and therefore we have made calculations also for the singly negative Ga and As vacancies by the LMTO-ASA Green function method, which is able to describe these states self-consistently. The dependence of the positron lifetime on the charge state is, however, weak in this model, which ignores the changes in the lattice relaxation. This result has also been obtained previously [12].

Experimental results for positron lifetimes at vacancies are given in table 4, too.

Table 4. Positron lifetimes for vacancies in Al and GaAs. The present theoretical results with self-consistent (τ_{SC}^{LDA}) and non-self-consistent (τ_{NSC}^{LDA}) electron structures are compared with those (τ^{cv}) obtained by calculating the core and valence annihilation rates separately. The self-consistent calculations are performed by the LMTO-ASA-Green's function method whereas the non-self-consistent results are obtained by the three-dimensional superimposed atom method. The experimental (τ^{exp}) positron lifetimes are also shown. The charge states of the Ga and As vacancies in experiments are non-positive, but otherwise uncertain.

Vacancy	τ_{SC}^{LDA} (ps)	τ_{NSC}^{LDA} (ps)	τ^{cv} (ps)	τ^{exp} (ps)
V_{Al}	247	245	253[a]	240[b]
V_{Ga}^{0}	262	254	265[c]	260[d]
V_{Ga}^{-1}	263			
V_{As}^{0}	263	256	268[c]	295[e]
V_{As}^{-1}	265			260[e]

[a][7]. [b][25]. [c][13]. [d][26]. [e][27].

The experimental positron lifetime of 240 ps (BaF_2 scintillators) [25] in the Al vacancy is slightly shorter than the theoretical results. According to the measurements, a positron lifetime of 260 ps is connected with the Ga vacancy [26] whereas two lifetimes of 260 ps and 295 ps are connected with the As vacancy [27]. The positron lifetime at the As vacancy is explained as decreasing when the charge state of the vacancy becomes more negative [27]. Thus on the basis of the present results the experimental lifetime components of 260 ps can be explained to arise from vacancies where the open volume for the positron is similar to the open volume in an unrelaxed vacancy. The positron lifetime of 295 ps would require a rather large relaxation increasing the open volume [28]. As the main conclusion from the comparison of the different theoretical and experimental positron lifetimes for vacancies we can state that the superimposed atom calculations employing non-self-consistent electron densities already give a rather good description for positron annihilation. Self-consistent electron structures are needed for the investigations of smaller details. On the other hand, the use of non-self-consistent electron densities gives smaller positron binding energies to defects than the use of self-consistent ones [12, 13]. Therefore in the case of very low binding energies, the use of self- consistent electron structures may be crucial.

Comparing the theoretical and experimental positron lifetimes it is evident that LDA describes the electron enhancement at the positron site surprisingly well, at least in the sense that the total annihilation rates or the positron lifetimes are rather well reproduced. A similar situation is met in the case of electron structure calculations, in which the LDA is used for electron exchange and correlation effects [1]. The success of the LDA in electron structure calculations has been argued to arise from constraints to the exchange–correlation hole around an electron in the electron gas [29]. Namely, the spatial integral over the exchange–correlation hole has to yield the lack of exactly one electron from the hole. Moreover, the exchange–correlation energy can be calculated so that the hole density is first spherically averaged. Therefore an isotropic LDA hole is not a bad approximation even in an inhomogeneous electron gas, in which the true exchange–correlation hole can be strongly anisotropic. The counterpart of the exchange–correlation hole in the case of a positron in an electron gas is the screening cloud around it. This screening cloud has to meet restrictions, too. Its spatial integral

has to obey the sum rule (equation (6)), which for the metals amounts to exactly one electron. Moreover, the form of the screening cloud at the positron is restricted by the cusp condition. Finally, the LDA for positrons should be more favoured than the LDA for electrons, because the positron in a lattice samples predominantly the interstitial regions where the density variations are much slower than in the core regions, which are important for electrons.

4. Conclusions

We have shown in this work that *ab-initio* calculations of positron lifetimes for all metals are possible within the LDA. If self-consistent electron structures are used, the calculated lifetimes agree rather well with experiments. In the case of transition metals the lifetimes are maybe slightly too short. Using a semiempirical model for the band gap induced reduction of electronic screening, reliable predictions for positron lifetimes are possible also for semiconductors. The present theoretical *ab-initio* results allow detailed studies of trends in positron annihilation rates along the rows and columns of the Periodic Table and thereby complete our similar systematic work [9] on the energetics of positrons in metals. Of the future applications of the scheme, positron studies of metallic alloys, in which several phases may exist segregated from each other, look very appealing. For these studies the knowledge of positron lifetimes as well as the affinities (energetics) for different phases is crucial.

For the systems studied in this work, with the exception of alkaline metals and semiconductors, methods using non-self-consistent electron structures give similar positron lifetimes to the ones employing self-consistent electron structures. This is due to the effect that the positron density relaxes following the electron density. Therefore in many practical applications, especially in those in which one is interested in the changes of the positron lifetime due to trapping at defects, the use of self-consistent electron structures is not necessary. In order to obtain reasonable estimates in these cases use of the three-dimensional superimposed atom method [7] is much more efficient than the use of the often very time-consuming self-consistent electron structure calculation methods.

References

[1] For a recent review see
Jones R O and Gunnarsson O 1989 *Rev. Mod. Phys.* **61** 689

[2] For a review, see
Puska M J 1987 *Phys. Status Solidi* a **102** 11

[3] Boroński E and Nieminen R M 1986 *Phys. Rev.* B **34** 3820
Nieminen R M, Boroński E and Lantto L 1985 *Phys. Rev.* B **32** 1377

[4] For the electron–electron exchange–correlation functional we use the results of
Ceperley D M and Alder B J 1980 *Phys. Rev. Lett.* **45** 566
as parametrized by
Perdew J and Zunger A 1981 *Phys. Rev.* B **23** 5048
For the positron–electron correlation functional we use the parametrization given in [3].

[5] Jensen K O 1989 *J. Phys.: Condens. Matter* **1** 10595

[6] Daniuk S, Šob M, and Rubaszek A 1991 *Phys. Rev.* B **43** 2580

[7] Puska M J and Nieminen R M 1983 *J. Phys. F: Met. Phys.* **13** 333

[8] For a recent review, see
Andersen O K, Jepsen O and Šob M 1987 *Electronic Band Structure and Its Applications* ed M Yussouff (Heidelberg: Springer) p 1

[9] Puska M J, Lanki P and Nieminen R M 1989 *J. Phys.: Condens. Matter* **1** 6081

[10] Boev O V, Puska M J and Nieminen R M 1987 *Phys. Rev.* B **36** 7786
[11] Gunnarsson O, Jepsen O and Andersen O K 1983 *Phys. Rev.* B **27** 7144
[12] Puska M J, Jepsen O, Gunnarsson O and Nieminen R M 1986 *Phys. Rev.* B **34** 2695
[13] Puska M J, Mäkinen S, Manninen M and Nieminen R M 1989 *Phys. Rev.* B **39** 7666
[14] Nieminen R M 1983 *Positron Solid State Physics* ed W Brandt and A Dupasquier (Amsterdam: North-Holland)
[15] Glötzel D, Segall B and Andersen O K 1980 *Solid State Commun.* **36** 403
[16] Seeger A A, Banhart F and Bauer W 1989 *Positron Annihilation* ed L Dorikens-Vanpraet, M Dorikens and D Segers (Singapore: World Scientific) p 275
[17] Chang T, Yin D, Cao G, Wang S and Liang J *et al* 1987 *Nucl. Instrum. Methods Phys. Res.* 1987 A **256** 398
[18] Saarinen K unpublished
[19] Arponen J and Pajanne E 1985 *Positron Annihilation* ed P C Jain, R M Singru and K P Gopinathan (Singapore: World Scientific) p 21
[20] Šob M 1985 *Solid State Commun.* **53** 249, 255
[21] Bonderup E, Andersen J U and Lowy D N 1979 *Phys. Rev.* B **20** 883
[22] Brandt W and Reinheimer J 1971 *Phys. Lett.* **35A** 109
[23] Hansen H E, Nieminen R M and Puska M J 1984 *J. Phys. F: Met. Phys.* **14** 1299
[24] Wang Xiao-Gang and Zhang Hong 1990 *J. Phys.: Condens. Matter* **2** 7275
[25] Jackman J A, Hood G H and Schultz R J 1987 *J. Phys. F: Met. Phys.* **17** 1817
[26] Hautojärvi P, Moser P, Stucky M and Corbel C 1986 *Appl. Phys. Lett.* **48** 809
[27] Corbel C, Stucky M, Hautojärvi P, Saarinen K and Moser P 1988 *Phys. Rev.* B **38** 8192
[28] Mäkinen S and Puska M J 1989 *Phys. Rev.* B **40** 12523
[29] Gunnarsson O, Jonson M and Lundquist B I 1979 *Phys. Rev.* B **20** 3136